Received 12 December 2005
Revised 14 July 2006
Accepted 14 July 2006

Application and performance comparison of high-resolution central schemes for the black oil model

H. Naderan, M.T. Manzari and S.K. Hannani
Sharif University of Technology, Tehran, Iran

Abstract

Purpose – The purpose of this paper is to investigate the performance of a specific class of high-resolution central schemes in conjunction with the black oil models for hydrocarbon reservoir simulation.

Design/methodology/approach – A generalized black oil model is adopted, in which the solubility of gas in both oil and water and evaporation of oil are considered, leading to a system of equations prone to degeneracy. A computer code is generated and three test cases are solved to evaluate the performance of various schemes in terms of accuracy and discontinuity handling.

Findings – It is shown that, although some of the central schemes are highly sensitive to the choice of Courant-Friedrich-Levy (CFL) number and produce overly diffusive results, a certain type of this class is insensitive to the CFL number and can conveniently handle degenerate equations appearing in the reservoir simulation. The obtained results are compared with those available in the literature, showing merits of this class of schemes in complex reservoir simulation models.

Research limitations/implications – This paper gives the one-dimensional implementation of the above-mentioned schemes. Extension to higher dimensional black oil model is currently under development by the authors.

Practical implications – The specific class of high-resolution central schemes investigated here presents the same level of accuracy as more complicated numerical methods, yet keeping it much more simple, by avoiding Riemann solvers.

Originality/value – The high-resolution central scheme used in this work has been newly developed and applied to simple scalar hyperbolic equations. It has been adopted for the black oil for the first time.

Keywords Fluid dynamics, Flow, Oils, Modelling

Paper type Research paper

Introduction

Enhancing oil production has been one of the main concerns of reservoir engineers throughout the history of petroleum industry. With the advent of high speed computing, reservoir simulation has proven to be an invaluable tool to this end. Based on half-a-century of research, various flow models for reservoir simulation are in use today. These models range from simple single-phase (Aronofsky and Jenkins, 1954) to sophisticated multi-phase and multi-component compositional models (Class *et al.*, 2002).

Black oil is one of the most popular models among reservoir engineers. This is mainly because the model provides a reasonably general representation of the multi-component multi-phase flow in porous media while avoiding the necessity of

International Journal of Numerical Methods for Heat & Fluid Flow
Vol. 17 No. 7, 2007
pp. 736-753

0961-5539
DOI 10.1108/09615530710777985

using complicated phase equilibrium models. In practice, to simulate different reservoir exploitation scenarios, the black oil model must be coupled with some auxiliary sub-models for the fluid, rock and energy transfer.

Owing to the tendency towards more complex flow models and their corresponding sub-models, there is an ever increasing demand for more computational power. Besides, to accurately represent small features of size of tens of centimeters in a reservoir of dimensions of several hundred of kilometers, tens of millions of grid cells are normally required. The need for more complex models and more resolution, can push the computer resources to the limit and thus show the need for computationally efficient methods. Moreover, they highlight the importance of the quest for more accurate computational methods.

Using a black oil model for reservoir simulation results in a system of degenerate, non-convex hyperbolic equations for component transport. The degeneracy comes from the fact that in some situations, although all of the chemical species are present, riot all of the expected phases coexist. This situation is termed as under saturation. Depending on the model used, one or several cases of under saturation may be present in the problem. Solution of such a system of equations which constantly switches between different degenerate cases is a challenging problem. Compared to the overwhelming amount of research and developed methods for the solution of strictly hyperbolic equations, e.g. the Euler equations in the fluid dynamics, little work is done in the field of degenerate equations, occurring in reservoir simulation.

In the reservoir simulation context, methods based on the Godunov or approximate Riemann solution are popular because of their robustness in capturing discontinuities. Based on the work of Godunov (1959), this class of methods, assume a piecewise constant or linear reconstruction of the solution variable and solve a local Riemann problem for every discontinuity, to advance the solution. In the context of hydrocarbon reservoir simulation, Bell *et al.* (1986a) and Colella (1990) have discussed second-order Godunov methods for use in reservoir simulation. In a later work, Bell *et al.* (1986b) considered the effect of gravitational force on the solution of Riemann problem for the second-order Godunov methods applied to the black oil model. On the other hand, several flux corrected transport methods have been used for restricted cases of incompressible miscible flows by Boris and Book (1973), Christie and Bond (1985) and Zalesak (1979).

However, the computational cost of these methods is high due to the need for full characteristic decomposition of the Jacobian matrix and eigen vector calculations. In addition, many cases of eigen value deficiency arise in complex reservoir models, due to the degeneracy of the equations which require special care, both in analysis and implementation.

On the other side of the numerical method's spectrum, central schemes with added artificial diffusion have long been used in compressible flow simulations. The work of Friedrichs and Lax (1971) was the starting point of the central schemes. Their method is based on a piecewise constant approximation of the solution. Compared to the first-order Godunov method, however, it does not require eigen value and eigenvector decomposition. The use of central schemes have been abandoned for a long time due to their excessive numerical diffusion. Nevertheless, their relative simplicity, ease of implementation and computational efficiency, motivated researchers to develop high-resolution central schemes with artificial diffusion.

Nessyahu and Tadmor (1990) have recently introduced a second-order successor to the Lax-Friedrichs scheme which retains its main advantage of not needing an either exact or approximate Riemann solver. Their extension was based on a staggered grid. The method was extended to higher-orders by Liu and Tadmor (1998) and Huynh (1995) and to higher dimensions by Arminijon *et al.* (1995) and Jiang and Tadmor (1998). Also, Jiang *et al.* (1998) have introduced a non-staggered grid version of this method.

All the above mentioned schemes have an artificial viscosity of order $O(\Delta x^{2r}/\Delta t)$ where r is the order of the scheme. Hence, with small time-steps, the numerical diffusion becomes progressively high. To remedy this deficiency, several schemes have been introduced. Kurganov and Tadmor (2000) introduced a modification to the Nessyahu-Tadmor scheme, making its numerical diffusion of order $O(\Delta x^{2r-1})$. In particular, their semi-discrete form is capable of handling degenerate conservation laws, which makes the method attractive to the reservoir simulations.

Other types of high-resolution central schemes also exist. Two of the most popular are the convective-upwind split-pressure scheme due to Jameson (1995a, b) and the scheme of Liu and Osher (1998), both of them being semi-discrete and achieving high resolution without using a Riemann solver.

In simulating a problem with a complex physics on a general domain with large variations in physical properties and grid size, the maximum allowable time-step size for each cell to reach a stable solution varies considerably. Setting the global time-step to the minimum of all cells makes the Courant-Friedrich-Levy (CFL) number for larger cells, smaller than the optimum value and the artificial diffusion becomes higher than expected. As a result, to ensure a good discontinuity capturing, a scheme should have an artificial diffusion independent of the CFL number. This property of the computational scheme is by no means trivial, and as will be shown in this work, schemes which do not possess this property, are not suitable for reservoir simulations, failing to capture the sharp fronts present in the solution.

In this work, the applicability of Nessyahu-Tadmor and Kurganov-Tadmor high-resolution central schemes to the black oil model is investigated. Also, a comparison with the traditional first-order Lax-Friedrichs scheme is performed. In the following, first a brief review of the governing equations of the black oil model is given and then important aspects of the numerical method are described. Finally, three one-dimensional benchmark problems are solved and some concluding remarks are presented.

Governing equations

Equations governing the black oil model can be formulated in several forms. The form chosen for the present work is based on the work of Trangenstein and Bell (1989), which uses a volume error discrepancy for derivation of the pressure equation. For the sake of brevity, the details of the assumptions and derivation process are not discussed here and only a brief review of the equations is presented.

In the black oil model, the reservoir fluid is considered to be composed of three pseudo-components, which are oil, gas and water, distributed into three phases, liquid, vapor and aqua. Neglecting the capillary effects, all phases will have the same pressure, p. The mass of components per pore volume is represented by the vector $\mathbf{z} = \{z_o, z_g, z_w\}^T$ and the volume of each phase by $\mathbf{u} = \{u_l, u_v, u_a\}^T$.

The pressure variation inside the reservoir is governed by the a parabolic equation:

$$\left(-\phi \mathbf{e}^T \frac{\partial u}{\partial p} + \mathbf{e}^T \mathbf{u} \frac{\partial \phi}{\partial p}\right) \frac{\partial p}{\partial t} + \mathbf{e}^T \mathbf{u} \frac{\partial u}{\partial z} \nabla \cdot (\mathbf{R}\mathbf{B}^{-1} \mathbf{v}_t) = \frac{\mathbf{e}^T \mathbf{u} - 1}{\Delta t} \phi \tag{1}$$

The vector of velocities is defined as:

$$\mathbf{v} = \begin{Bmatrix} \mathbf{v}_l^T \\ \mathbf{v}_v^T \\ \mathbf{v}_a^T \end{Bmatrix}$$

in which:

$$\mathbf{v}_j = -\lambda_j (\nabla p - \rho_j \mathbf{g})$$

are the phase velocities and $\mathbf{v}_t = \mathbf{v}^T \mathbf{e}$ is the total velocity. Moreover, $\mathbf{e} = \{1, 1, 1\}^T$, ϕ is the porosity, ρ_j is density of phase j, $\mathbf{g}$ is the gravitational acceleration vector and t is time. Also, $\lambda_j = K k_{r_j} / \mu_j$ is the mobility of phase j where K is the rock permeability, and k_{r_j} and μ_j are the relative permeability and dynamic viscosity of phase j, respectively.

The matrix $\mathbf{B} = \text{diag}\{B_l, B_v, B_a\}$, is the volume formation factor which shows the volume of each phase in reservoir condition compared to the Stock Tank Condition (STC). In the absence of thermal effects, B_l, B_v and B_a are functions of the phase pressure.

The matrix $\mathbf{R}$ is the solution ratio. R_{ij} is defined as the amount of component i in phase j, compared to the amount of principal component of phase j. The principal component of a phase is, by definition, the component present in that phase at STC. Specifically, oil, gas and water are the principal components of the liquid, vapor and aqua phases, respectively.

In the classical black oil model, only the solubility of gas in oil is considered, giving the $\mathbf{R}$ matrix the following structure:

$$\mathbf{R} = \begin{bmatrix} 1 & 0 & 0 \\ R_l & 1 & 0 \\ 0 & 0 & 1 \end{bmatrix} \quad R_l = \frac{z_{gl}}{z_{ol}} \tag{2}$$

where z_{ij} is the mass of component i in phase j per pore volume. The model considered by Trangenstein and Bell (1989) is rather more general and considers the solubility of gas in both oil and water and evaporation of oil, with the following $\mathbf{R}$ matrix:

$$\mathbf{R} = \begin{bmatrix} 1 & R_v & 0 \\ R_l & 1 & R_a \\ 0 & 0 & 1 \end{bmatrix} \quad R_l = \frac{z_{gl}}{z_{ol}} \quad R_v = \frac{z_{ov}}{z_{gv}} \quad R_a = \frac{z_{ga}}{z_{wa}} \tag{3}$$

In this work, the general model of Trangenstien and Bell is adopted. The transport of components is governed by the mass conservation law which yields:

$$\frac{\partial \phi \mathbf{z}}{\partial t} + \nabla \cdot (\mathbf{R}\mathbf{B}^{-1}\mathbf{v}) = 0 \tag{4}$$

Here, $\mathbf{u}$ and $\mathbf{z}$ are related together by:

$$\mathbf{u} = \mathbf{B}\mathbf{T}\mathbf{z} \tag{5}$$

where $\mathbf{T}$ is a matrix such that $\mathbf{T}\mathbf{R} = \mathbf{I}$.

When all the three phases are present, the flow is termed saturated. However, there is a possibility that all the gas is dissolved into the liquid phase, thus, eliminating the vapor phase. This situation is called under-saturation which shows that the reservoir pressure is higher than the liquid bubble pressure and the liquid phase has the capacity to swallow more gas. In this case, $\mathbf{R}$, $\mathbf{T}$ and $\mathbf{B}$ matrices need to be modified but the general form of equations (1), (4) and (5) does not alter. This is the main reason for choosing this formulation as the base of present work, since it permits a unified treatment of the saturated and under-saturated cases. For a detailed discussion of the under-saturated cases, consult Trangenstein and Bell (1989).

Numerical method

A finite volume approach was chosen for the discretization of equations (1) and (4). For a domain of length L, the one-dimensional grid is defined by:

$$x_i = (i-1)\Delta x \quad i = 1, 2, \ldots, n \quad \Delta x = \frac{L}{n-1} \tag{6}$$

The control volume corresponding to node i is the space enclosed by faces i-1/2 and $i + 1/2$. Integrating equation (1) on control volume i gives:

$$\iint \alpha \frac{\partial p}{\partial t}\, \mathrm{d}x\mathrm{d}t + \iint \mathbf{e}^T \mathbf{B}\mathbf{T} \frac{\partial}{\partial x}(\mathbf{R}\mathbf{B}^{-1}\mathbf{v})\, \mathrm{d}x\mathrm{d}t = \iint \beta\, \mathrm{d}x\mathrm{d}t \tag{7}$$

where:

$$\alpha = -\phi \mathbf{e}^T \frac{\partial \mathbf{u}}{\partial p} + \mathbf{e}^T \mathbf{u} \frac{\partial \phi}{\partial p} \quad \beta = \frac{\mathbf{e}^T \mathbf{u} - 1}{\Delta t}\, \phi$$

Assuming that p is constant over the control volume, $\mathbf{R}\mathbf{B}^{-1}$in the second term comes out of the derivative simplifying equation (7) to the following equation:

$$\alpha_i \left(p_i^{n+1} - p_i^n\right)\Delta x + \Delta t \left[{v_t^{n+1}}_{i+1/2} - {v_t^{n+1}}_{i-1/2} \right] = \beta_i \Delta x \Delta t \tag{8}$$

The coefficients α and β are evaluated at time t_n while the total velocities are evaluated at time t_{n+1} making the pressure equation implicit. The vector notation for the total velocity is not used, since the equation is written for a one-dimensional model.

For the component transport, integration over the control volume using an explicit time approximation gives:

$$\mathbf{z}_i^{n+1} - \mathbf{z}_i^n = -\frac{\Delta t}{\phi_i \Delta x} \left[\mathbf{h}_{i+1/2} - \mathbf{h}_{i-1/2} \right] \tag{9}$$

where $\mathbf{h}_{i+1/2}$ is the flux vector $\mathbf{RB}^{-1}\mathbf{v}$ evaluated over the face $i + 1/2$. It can be written as a function of the conserved variables on the two sides of the face. Below three variants of the central scheme family are presented.

Lax-Friedrichs scheme

The first-order Lax-Friedrichs scheme has an artificial diffusion of order $O(\Delta x^2/\Delta t)$. The numerical flux is written as:

$$\mathbf{h}_{i+1/2} = \frac{1}{2}\left[\mathbf{h}_{i+1} + \mathbf{h}_i\right] - \frac{1}{4\tau}\left(\mathbf{z}_{i+1} - \mathbf{z}_i\right) \tag{10}$$

in which $\tau = \Delta t/\Delta x$ and $\mathbf{h}_i = \mathbf{h}(\mathbf{z}_i)$.

Nessyahu-Tadmor scheme

The scheme presented by Nessyahu and Tadmor (1990) is a second-order accurate method which uses staggered grid. Here, the non-staggered version introduced by Jiang *et al.* (1998) is employed. The artificial diffusion of this method is of $O(\Delta x^4/\Delta t)$. The flux function is given by:

$$\mathbf{h}_{i+1/2} = \frac{1}{2}\left[\mathbf{h}_{i+1}^{n+1/2} + \mathbf{h}_i^{n+1/2}\right] - \frac{1}{4\tau}(\mathbf{z}_{i+1} - \mathbf{z}_i) + \frac{\Delta x}{16\tau}\left[\mathbf{z}'_{i+1} + \mathbf{z}'_i\right] + \frac{\Delta x}{8\tau}\mathbf{z}'_{i+1/2} \tag{11}$$

where:

$$\mathbf{z}'_i = MM\left(\frac{\mathbf{z}_{i+1} - \mathbf{z}_i}{\Delta x}, \frac{\mathbf{z}_i - \mathbf{z}_{i-1}}{\Delta x}\right) \quad \mathbf{z}'_{i+1/2} = MM\left(\frac{\Delta \mathbf{z}_{i+1}^{n+1}}{\Delta x}, \frac{\Delta \mathbf{z}_i^{n+1}}{\Delta x}\right) \tag{12}$$

and:

$$\Delta \mathbf{z}_i^{n+1} = \frac{\mathbf{z}_{i+1}^n - \mathbf{z}_{i-1}^n}{2} - \frac{\Delta x}{8}\left(\mathbf{z}'_{i-1} - 2\mathbf{z}'_i + \mathbf{z}'_{i+1}\right) - \tau\left[\mathbf{h}_{i-1}^{n+1/2} - 2\mathbf{h}_i^{n+1/2} + \mathbf{h}_{i+1}^{n+1/2}\right]$$

The term $\mathbf{h}_i^{n+1/2}$ is evaluated at:

$$\mathbf{z}_i^{n+1/2} = \mathbf{h}_i^n - \frac{\tau}{2}\frac{\partial \mathbf{h}}{\partial x}\Delta t$$

$MM(x,y)$ is the minmod limiter and is defined as:

$$MM(x,y) = \begin{cases} \min(x,y) & x > 0 \text{ and } y > 0 \\ \max(x,y) & x < 0 \text{ and } y < 0 \\ 0 & xy < 0 \end{cases} \tag{13}$$

It should be noted that in the above equations, $\mathbf{z}'_i$ and $\mathbf{z}'_{i\pm1/2}$ are evaluated at t^n and t^{n+1}, respectively.

Kurganov-Tadmor scheme

Kurganov and Tadmor (2000) has formulated his method in both semi- and fully-discrete forms. Here, the semi-discrete form is used since it is already in the conservation form. Nevertheless, the same expression for face flux can be reached from

the fully-discrete form with some algebraic manipulations. This method has an artificial diffusion of order $O(\Delta x^3)$. The numerical flux is given by:

$$\mathbf{h}_{i+1/2} = \frac{1}{2}\left[\mathbf{h}^{+}_{i+1/2} + \mathbf{h}^{-}_{i+1/2}\right] - \frac{1}{2}\, a_{i+1/2}\left(\mathbf{z}^{+}_{i+1/2} - \mathbf{z}^{-}_{i+1/2}\right) \tag{14}$$

in which:

$$\mathbf{z}^{+}_{i+1/2} = \mathbf{z}_{i+1} - \frac{\Delta x}{2}\mathbf{z}'_{i+1} \quad \mathbf{z}^{-}_{i+1/2} = \mathbf{z}_{i} + \frac{\Delta x}{2}\mathbf{z}'_{i}$$

are the right and left states, respectively, and $\mathbf{h}^{\pm}_{i+1/2} = \mathbf{h}(\mathbf{z}^{\pm}_{i+1/2})$. The variable derivatives are evaluated using the same minmod limiter. The wave speed at cells' interface, $a_{i+1/2}$ is defined as:

$$\rho\left(\frac{\partial \mathbf{h}}{\partial z}(\mathbf{z})\right) \quad \mathbf{z} \in \mathscr{C}\left(\mathbf{z}^{-}_{i+1/2}, \mathbf{z}^{+}_{i+1/2}\right)$$

where $\rho(\mathbf{A})$ is the spectral radius of matrix $\mathbf{A}$ and $\mathscr{C}(\mathbf{z}^{-}_{i+1/2}, \mathbf{z}^{+}_{i+1/2})$ is a path that connects the two states $\mathbf{z}^{-}_{i+1/2}$ and $\mathbf{z}^{+}_{i+1/2}$ in the phase space via Ricmann fans.

Since, the flux function is non-convex and complicated to evaluate, it is not easy to find $a_{i+1/2}$ accurately. In the present work, the following estimate is used:

$$a_{i+1/2} = \rho\left(\frac{\partial \mathbf{h}}{\partial \mathbf{z}}(\bar{\mathbf{z}})\right) \tag{15}$$

in which $\bar{\mathbf{z}}$ is the arithmetic mean of $\mathbf{z}^{-}_{1+1/2}$ and $\mathbf{z}^{+}_{1+1/2}$. Numerical experiments proved that this is sufficiently close to the true maximum wave speed.

The CFL condition for the three schemes is computed on the basis of a and a global CFL number, C, at each face, using:

$$\frac{a\Delta t}{\Delta x} < C \tag{16}$$

In practice, a global time-step size is used which is the minimum allowable time-step computed for all computational cells.

Tests, results and discussion

To assess the performance of the above mentioned numerical methods, three test cases were solved. The results for each test case consist of the solution of the problem by three methods, Lax-Friedrichs, Nessyahu-Tadmor and Kurganov-Tadmor, abbreviated by LF, NT and KT, respectively.

The first benchmark is the so-called two-phase Buckley-Leverett problem which is widely used in the field of reservoir engineering. The second and third benchmarks were adapted from Trangenstein and Bell (1989). Since, a higher-order Godunov scheme was used in Trangenstein and Bell (1989), the solutions in the current work will also be illuminating, in comparing the results obtained from central and Godunov schemes. In order to compare the results of test case 2 and 3, the fluid and rock properties are taken as those given in Trangenstein and Bell (1989), which are given in the Appendix.

The first problem, as stated, is a two-phase water flooding problem. Although the problem is two-phase and can be solved by defining a scalar flux, this was not done here and the full black oil model was used instead, with the gas component set to zero. Though the physics is simplified, the numerical complexities of the black oil model still exist. The initial reservoir and injection compositions are:

$$\mathbf{z}_{res} = \begin{Bmatrix} 1.0 \\ 0.0 \\ 0.0 \end{Bmatrix} \quad \mathbf{z}_{inj} = \begin{Bmatrix} 0.0 \\ 0.0 \\ 1.0 \end{Bmatrix} \tag{17}$$

A constant pressure $p = 0$ and total velocity $v_t = 0.1$ were applied to the domain $0 \leq x \leq 1$. This situation, essentially circumvents the solution of the pressure equation and tests the performance of different flux estimation methods in the component transport equation.

In this test case, the expected profile is the Buckley-Leverett solution. In this test case a mobility ratio equal to 1 was used so the front tip should be at $S_w = 0.7$. The problem was solved for CFL number equal to 0.4, 0.1 and 0.02. The results are given for three different times. The LF scheme (Figure 1) has a large artificial diffusion, even at large CFL numbers, but at shape of the solution is correct. This was expected in advance since the method is only first-order accurate. As the CFL number is reduced, however, the situation worsens arid the increasingly higher numerical diffusion completely wipes out the shock front at CFL $= 0.02$.

The NT scheme (Figure 2) provides a much better resolution for the shock front at CFL $= 0.4$ since it is second-order accurate. But the solution quality degrades as the CFL number is reduced, which is an indication of the inverse proportionality of the numerical diffusion and the time-step size on a fixed sized grid.

The KT scheme (Figure 3) gives virtually the same result regardless of the CFL number, which indicates its independency of the time-step size variation.

Figure 4 shows the progress of the front for the three schemes. At CFL $= 0.4$ the KT scheme shows a marginally smaller diffusion compared to NT scheme, which is due to its smaller constant coefficient in the numerical diffusion term. For NT, this coefficient is 1.0 while for KT it is $\Delta t/\Delta x$.

The second test case involves injection of a saturated mixture into a saturated black oil reservoir. The initial reservoir pressure is 1,800 psi and injection and production takes place at 2,000 and 1,600 psi, respectively. This test case signifies the effect of composition variation on the flow. The domain is defined as $0 \leq x \leq 1000$ and the initial reservoir and injection compositions are:

$$\mathbf{z}_{res} = \begin{Bmatrix} 0.703 \\ 70.3 \\ 0.0502 \end{Bmatrix} \quad \mathbf{z}_{inj} = \begin{Bmatrix} 0.0414 \\ 66.23 \\ 0.497 \end{Bmatrix} \tag{18}$$

For this test case, no analytical solution exits. Trangenstein and Bell (1989) have shown that the solution consists of two wave fronts, one slow-running between the oil and water components and one fast-running between the gas and oil components. The problem was solved on a 200-node grid and with a CFL equal to 0.45 and 0.1.

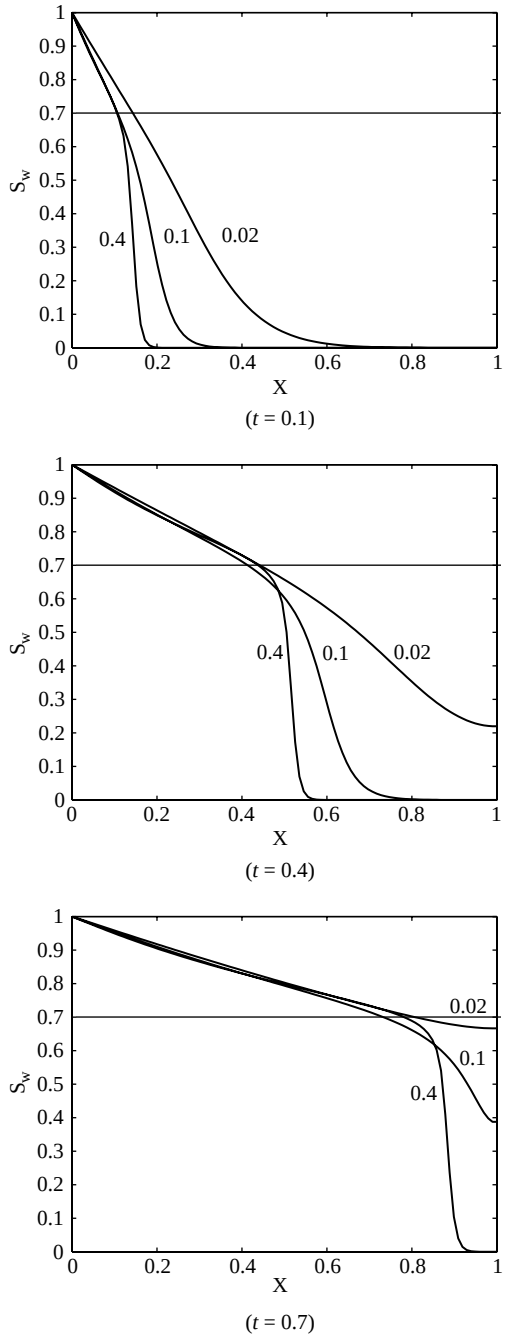

Figure 1.
Test case 1: water saturation profiles obtained by the LF scheme at various times

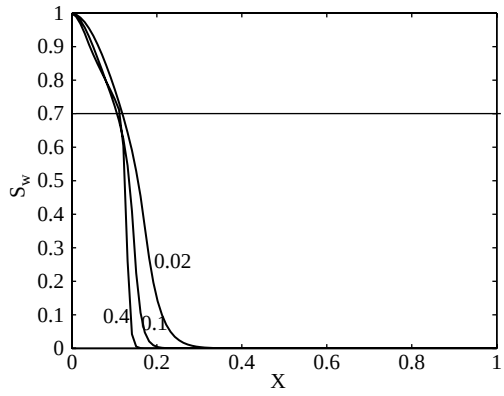

(t = 0.1)

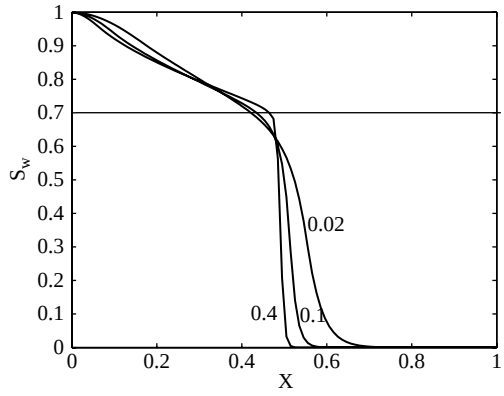

(t = 0.4)

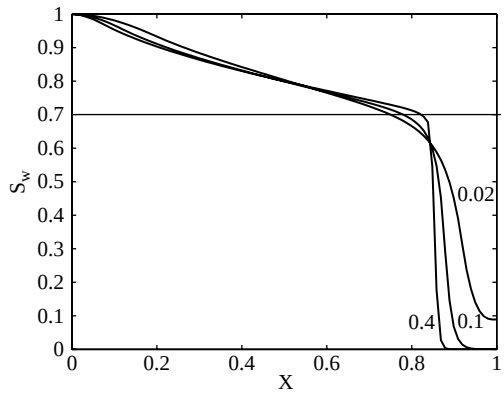

(t = 0.7)

Figure 2.
Test case 1: water saturation profiles obtained by the NT scheme at various times

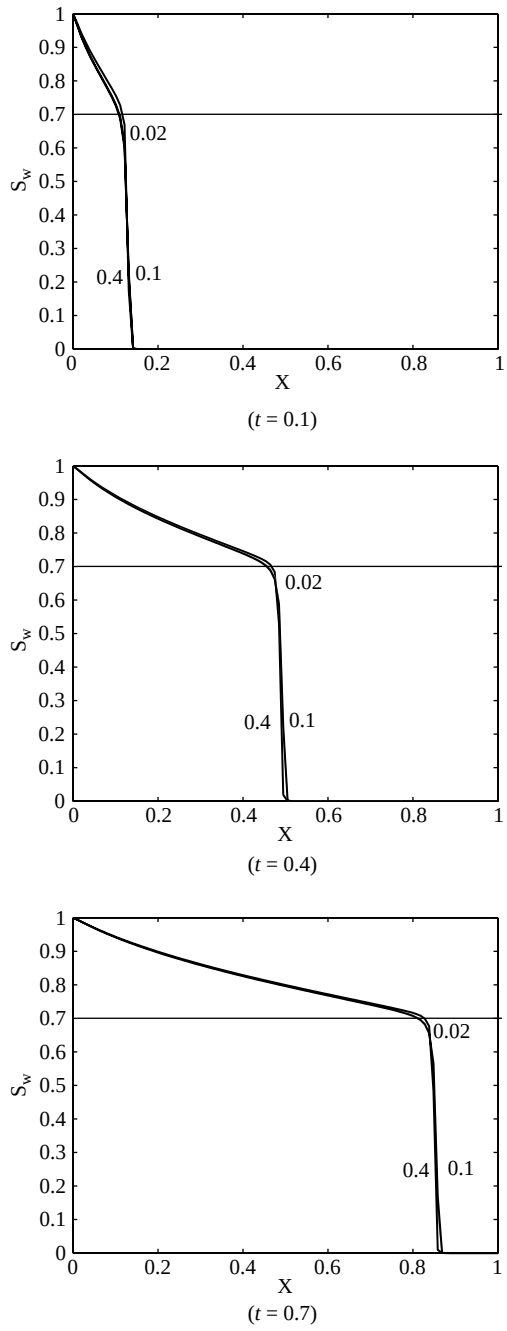

Figure 3.
Test case 1: water saturation profiles obtained by the KT scheme at various times

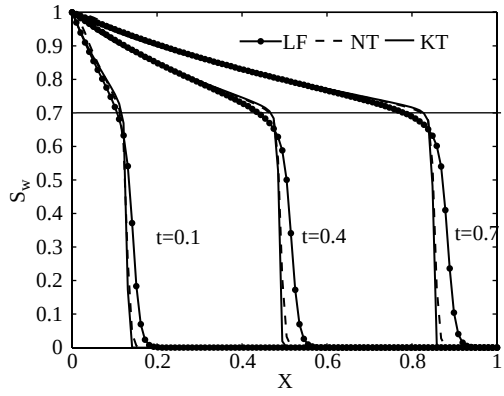

(CFL = 0.4)

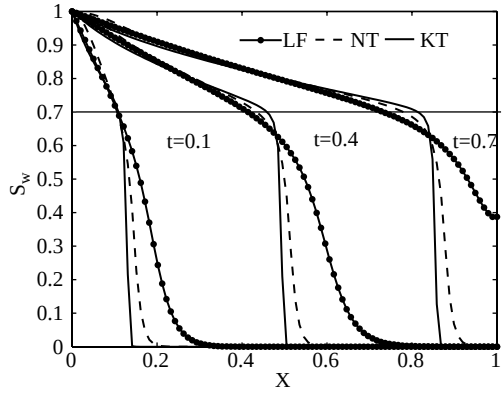

(CFL = 0.1)

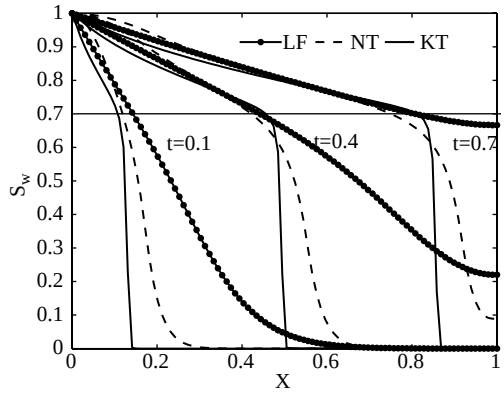

(CFL = 0.2)

Figure 4.
Progress of the three schemes through time, compared to each other

The results obtained by LF method is too diffuse (Figure 5). Although the CFL number was set to the maximum permissible value, the front is smeared. At reduced CFL number the front totally vanishes.

The NT scheme performs well at high CFL numbers (Figure 6) even though the fronts are not as sharp as the ones with KT scheme (Figure 7). The quality of its front

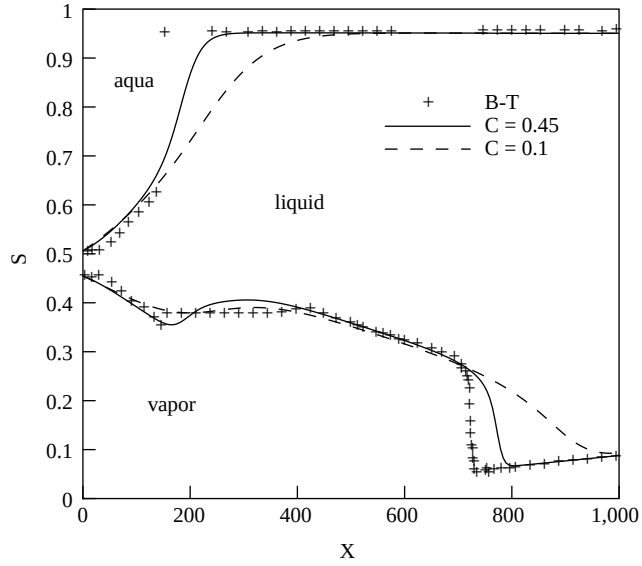

Figure 5.
Test case 2: saturation profiles obtained by the LF scheme, Time = 150 days

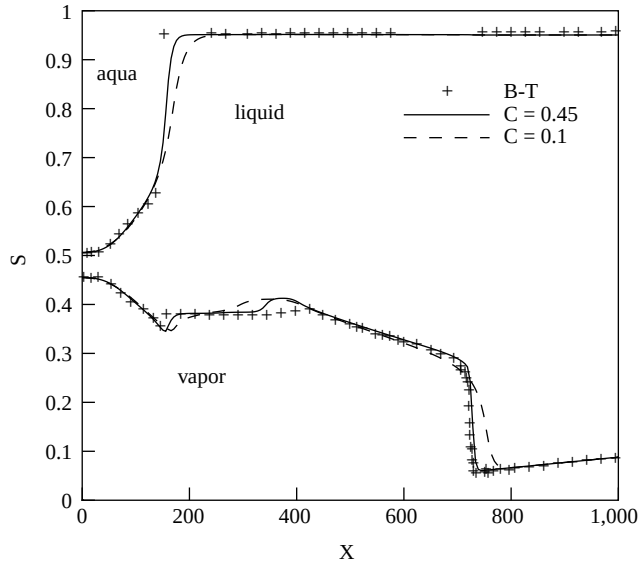

Figure 6.
Test case 2: saturation profiles obtained by the NT scheme, Time = 150 days

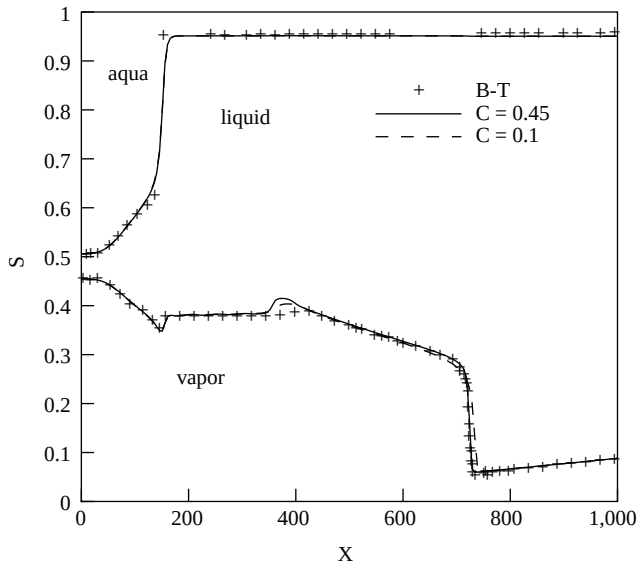

Figure 7.
Test case 2: saturation profiles obtained by the KT scheme, Time = 150 days

degrades rapidly as the CFL number is reduced. By contrast, the results obtained from the KT scheme at different CFL numbers, coincide on each other, which is remarkable, compared to the other two methods.

The third test case is the water flooding of an under-saturated oil reservoir. The initial reservoir, injection and production pressures are 3,500 psi, 4,000 psi and 3,000 psi, respectively. This test case shows the effect of pressure variation on the flow and composition. The domain is the same as test case two and the initial reservoir and injection compositions are:

$$\mathbf{z}_{res} = \begin{Bmatrix} 0.646 \\ 116.29 \\ 0.0 \end{Bmatrix} \quad \mathbf{z}_{inj} = \begin{Bmatrix} 0.0 \\ 0.0 \\ 1.27 \end{Bmatrix} \tag{19}$$

Like the previous test case, there is no analytical solution for the third test case. As expected, the solution exhibits a front between water and oil which starts from the injection well and progresses towards the production well. As the reservoir pressure drops, near the production well, the flow becomes saturated and free gas is produced, which introduces another front. Figures 8-10 show the results for a grid with 200 points and with CFL equal to 0.45 and 0.1. The figures compare the performance of the three methods which show the same trend as the previous two cases.

As it is shown in the obtained results, the classical Lax-Friedrichs scheme must be excluded from the selection set, because it is first-order accurate with an unacceptably high amount of artificial diffusion. The Nessyahu-Tadmor scheme has better performance in terms of artificial diffusion, since it is of second-order accuracy. However, its advantage is limited to high CFL numbers. As the CFL number decreases, the numerical diffusion starts to grow, diminishing the accuracy of the solution. On the

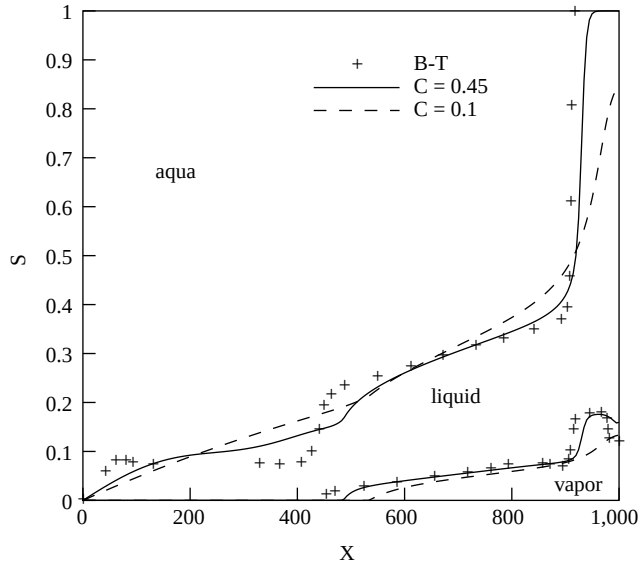

Figure 8.
Test case 3: saturation profiles obtained by the LF scheme, Time = 125 days

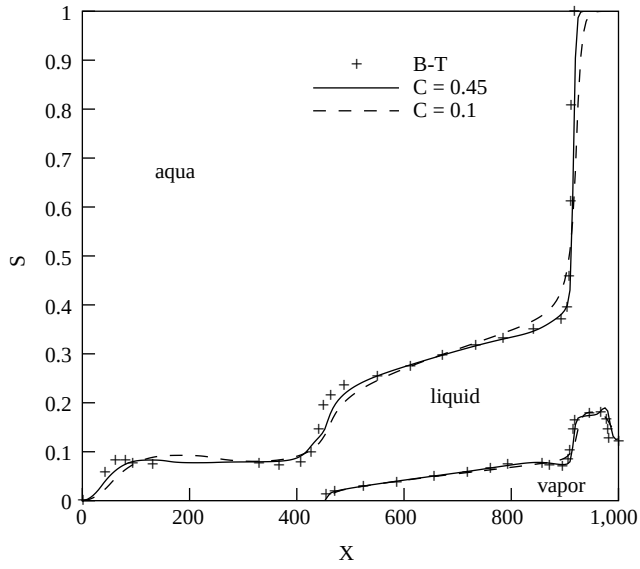

Figure 9.
Test case 3: saturation profiles obtained by the NT scheme, Time = 125 days

contrary, the Kurganov-Tadmor does not exhibit this flaw, being robust and accurate at any CFL number. Based on the facts mentioned in the introduction section and the results obtained here, it is seen that the KT scheme can be a favorable scheme for black oil simulations.

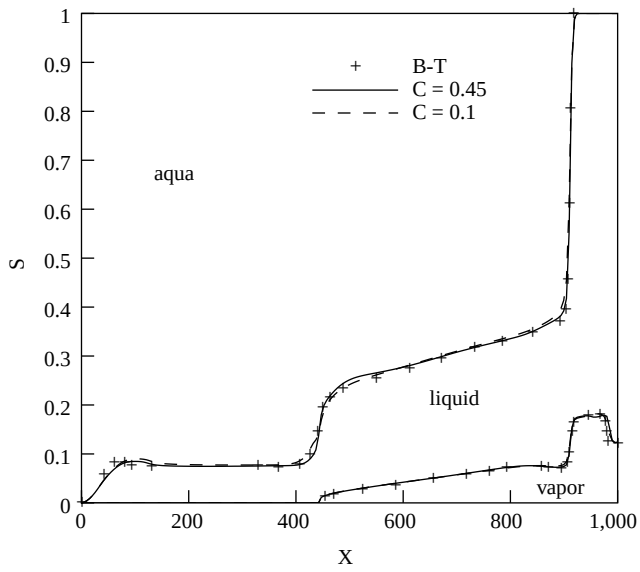

Figure 10.
Test case 3: saturation profiles obtained by the KT scheme, Time = 125 days

Conclusion

In this work, the possibility of application of high-resolution central schemes to the black oil model was investigated. The obtained results showed that methods whose artificial diffusion were independent of the time-step size offered a far superior resolution for complex simulations, especially in cases where a reduction of CFL number was necessary due to practical reasons. As an example, it was shown that the second-order NT method suffers from an excessive numerical diffusion at lower CFL numbers. Specifically, from the three methods investigated here, only the one proposed by Kurganov and Tadmor showed promising results for the black oil model. The method retains its accuracy, exhibits CFL independency and shows good capability in handling degenerate equations.

References

Arminijon, P., Stanescu, D. and Viallon, M.C. (1995), "A two-dimensional finite volume extension of the Lax-Friedrics and Nessyahu-Tadmor schemes for compressible flow", in Hafez, M. (Ed.), *Proceedings of the 6th International Symposium on CFD, Lake Tahoe*,Vol. 4, pp. 7-14.

Aronofsky, J.S. and Jenkins, R. (1954), "A simplified analysis of unsteady radial gas flow", *Transactions of AIME*, Vol. 201, pp. 149-54.

Bell, J.B., Shubin, G.R. and Trangenstein, J.A. (1986a), "A method for reducing numerical dispersion in two-phase black-oil reservoir simulation", *Journal of Computational Physics*, Vol. 65, pp. 71-106.

Bell, J.B., Trangenstein, J.A. and Shubin, G.R. (1986b), "Conservation laws of mixed type describing three phase flow in porous media", *SIAM Journal of Applied Mathematics*, Vol. 46, pp. 1000-17.

Boris, J.P. and Book, D.L. (1973), "Flux corrected transport 1: SHASTA a fluid transport algorithm that works", *Journal of Computational Physics*, Vol. 11, pp. 38-69.

Christie, M.A. and Bond, D.J. (1985), "Multidimensional flux corrected transport for reservoir simulation", paper presented at 8th SPE Symposium on Reservoir Simulation, Dallas, Texas, pp. 81-90.

Class, H., Helmig, R. and Bastian, P. (2002), "Numerical simulation of non-isothermal multiphase multicomponent processes in porous media", *Advances in Water Resources*, Vol. 25 No. 5, pp. 533-50.

Colella, P. (1990), "Multidimensional upwind methods for hyperbolic conservation laws", *Journal of Computational Physics*, Vol. 87, pp. 171-200.

Friedrichs, K.O. and Lax, P.D. (1971), "Systems of conservation equations with a convex extension", *Proceedings of the National Academy of Science, USA*, Vol. 68, pp. 1686-8.

Godunov, K.S. (1959), "A finite difference method for the numerical computation of discontinuous solutions of the equations of fluid dynamics", *Matematicheskii Sbornik*, Vol. 47, pp. 271-90.

Huynh, H.T. (1995), "A piecewise-parabolic dual-mesh method for the Euler equations", paper presented at 12th AIAA Computational Fluid Dynamics Conference, pp. 1054-66.

Jameson, A. (1995a), "Analysis and design of numerical schemes for gas dynamics 1 artificial diffusion, upwind biasing, limiters and their effect on accuracy and multigrid convergence", *International Journal of Computational Fluid Dynamics*, Vol. 4, pp. 171-218.

Jameson, A. (1995b), "Analysis and design of numerical schemes for gas dynamics 2 artificial diffusion and discrete shock structure", *International Journal of Computational Fluid Dynamics*, Vol. 5, pp. 1-38.

Jiang, G.S. and Tadmor, E. (1998), "Nonoscillatory central schemes for multidimensional hyperbolic conservation laws", *SIAM Journal on Scientific Computing*, Vol. 19, pp. 1892-917.

Jiang, G.S., Levy, D., Lin, C.T., Osher, S. and Tadmor, E. (1998), "High-resolution nonoscillatory central schemes with nonstaggered grids for hyperbolic conservation laws", *SIAM Journal on Numerical Analysis*, Vol. 35 No. 6, pp. 2147-68.

Kurganov, A. and Tadmor, E. (2000), "New high-resolution central schemes for nonlinear conservation laws and convection-diffusion equations", *Journal of Computational Physics*, Vol. 160, pp. 241-82.

Liu, X.D. and Osher, S. (1998), "Convex ENO high order multi-dimensional schemes without field by field decomposition or staggered grids", *Journal of Computational Physics*, Vol. 160, p. 304.

Liu, X.D. and Tadmor, E. (1998), "Third order nonoscillatory central scheme for hyperbolic conservation laws", *Numerical Mathematics*, Vol. 79, pp. 397-425.

Nessyahu, H. and Tadmor, E. (1990), "Non-oscillatory central differencing for hyperbolic conservation laws", *Journal of Computational Physics*, Vol. 87, pp. 408-63.

Trangenstein, J.A. and Bell, J.B. (1989), "Mathematical structure of the black-oil model for petroleum reservoir simulation", *SIAM Journal of Applied Mathematics*, Vol. 49 No. 3, pp. 749-83.

Zalesak, S. (1979), "Fully multidimensional flux corrected transport algorithms for fluids", *Journal of Computational Physics*, Vol. 31, pp. 335-62.

Appendix. Properties of rock and fluids

The spatial coordinate x has units of feet, and time t is measured in days. Pressure p is measured in psi, viscosity is measured in centipoise and the rock permeability K is measured in 0.006328 times the value in millidarcies. In this work, $K = 100md$ and porosity $\phi = 0.2(1 + 10^{-5}p)$.

The relative permeability functions are:

$$k_{r_l} = (1 - s_v - s_a)(1 - s_v)(1 - s_a) \quad k_{r_v} = s_v^2 \quad k_{r_a} = s_a^2$$

The solution ratios are given as:

$$R_l(p) = 0.05p \quad R_v(p) = 9 \times 10^{-5} - 6 \times 10^{-8}p + 1.6^{-11}p^2 \quad R_a(p) = 0.005p$$

Viscosities are defined by:

$$\mu_l = \begin{cases} 0.8 - 10^{-4}p & \text{saturated liquid} \\ (0.8 - 10^{-4}p_b)(1 + 6.78 \times 10^{-5}(p - p_b)) & \text{undersaturated liquid} \end{cases}$$

$$\mu_v = 0.012 + 3 \times 10^{-5}p$$

$$\mu_a = \begin{cases} 0.35 & \text{saturated aqua} \\ 0.35(1 + 6.78 \times 10^{-5}(p - p_b)) & \text{undersaturated aqua} \end{cases}$$

and finally, the volume formation factors are

$$B_l = \begin{cases} 1.0 - 2.31 \times 10^{-5}p & \text{if } R_l(p) \equiv 0 \\ 1.0 + 1.5 \times 10^{-4}p & \text{saturated liquid} \\ \dfrac{1.0 + 1.5 \times 10^{-4}p_b}{1.0 + 2.31 \times 10^{-5}(p - p_b)} & \text{undersaturated liquid} \end{cases}$$

$$B_v = \begin{cases} \dfrac{1}{6.0 + 0.06p} & \text{saturated vapor} \\ \dfrac{1}{7.0 + 0.06p} + \dfrac{\bar{R}_v}{R_v}\left[\dfrac{1}{6.0 + 0.06p} - \dfrac{1}{7.0 + 0.06p}\right] & \text{undersaturated vapor} \end{cases}$$

$$B_a = \begin{cases} 1.0 - 1.8 \times 10^{-5}p & \text{if } R_a(p) \equiv 0 \\ 1.0 - 3 \times 10^{-6}p & \text{saturated aqua} \\ \dfrac{1.0 - 3 \times 10^{-6}p_b}{1.0 + 1.8 \times 10^{-5}(p - p_b)} & \text{undersaturated aqua} \end{cases} \tag{20}$$

Corresponding author
M.T. Manzari can be contacted at: mtmanzari@sharif.edu